Biosensors and Bioelectronics 87 (2017) 242–248

Contents lists available at ScienceDirect

Biosensors and Bioelectronics

journal homepage: www.elsevier.com/locate/bios

Ultrasensitive, label-free detection of cardiac biomarkers with optical SIS sensor

Mangesh S. Diware [a], Hyun Mo Cho [a,*], Won Chegal [a], Yong Jai Cho [a], Dong Soo Kim [a,b], Sang Won O [a,c], Kyeong-Suk Kim [b], Se-Hwan Paek [c]

[a] Center for Nanometrology, Korea Research Institute of Standards and Science, Daejeon 305340, Republic of Korea
[b] Department of Mechanical System Engineering, Chosun University, Gwangju 61452, Republic of Korea
[c] Department of Bio-Microsystem Technology, Korea University, Seoul 02841, Republic of Korea

ARTICLE INFO

Article history:
Received 17 May 2016
Received in revised form
4 August 2016
Accepted 16 August 2016
Available online 18 August 2016

Keywords:
SIS sensors
Acute myocardial infarction
Troponin I
Myoglobin
CK-MB
Ellipsometry
Biosensors

ABSTRACT

Acute myocardial infarction (MI) is the leading cause of high mortality and morbidity rate worldwide, early and accurate diagnosis can increase the chances of survival. In this work, we report a simple, ultrasensitive, label-free, and high-throughput solution immersed silicon (SIS) immunosensor based on non-reflection condition (NRC) for *p*-polarized wave for early diagnosis of MI. SIS sensor chips are just a thin dielectric polymer layer on the silicon surface, which can be functionalized for specific application. At NRC, SIS sensors are extremely sensitive to the growing thickness of a bio-layer on the sensor surface while independent of refractive index change of the surrounding medium. Therefore, SIS signal is free from thermal noise, unlike surface plasmon resonance based sensor. Also, there is no need of reference signal which facilitates fast and accurate interaction measurement. Here, SIS technology is applied to tackle two issues in MI diagnosis: high sensitivity with the direct assay and the ability to measure in human serum. Myoglobin, creatine kinase-MB, and cardiac troponin I (cTnI) proteins were used as the MI biomarkers. We were able to measure over a broad concentration range with the detection limit of 5 and 10 pg/ml for cTnI in PBS and blood serum, respectively. The response time is about 5 min. This novel technique is a suitable candidate for cost effective point-of-care application.

1. Introduction

Acute myocardial infarction (MI), commonly called as heart attack, is irreversible damage to the heart cells caused by insufficient blood supply due to blockage in the coronary arteries. In 2012, cardiovascular diseases took nearly 17.5 million lives which were 31% of total global death, among them 7.4 million were due to coronary heart diseases and the number is growing (WHO, 2015). The MI diagnosis mostly relies on its symptoms of severe chest pain or any other anginal discomfort. However, nearly 28% of men and 35% of women do not show any of these symptoms (Gutterman, 2009), known as the silent MI, are at high risk. The most common tests include electrocardiography (ECG) (Richard et al., 2012; Ahmed et al., 2007) and magnetic resonance imaging (Ahmed et al., 2013) in combination with the stress test. These methods suffer several disadvantages such as non-specificity of ST segment changes in ECG, the need of skilled technician, human error source, and time-consuming. Early, accurate, and fast diagnosis can improve risk stratification and treatment, especially during perioperative procedures, which could increase the survival rate.

Certain proteins are released into the bloodstream when heart muscles get damaged, known as cardiac biomarkers. Recognition, quantification, and temporal behavior of these markers proven to be a best noninvasive tool for MI diagnosis (Janota, 2014; Jaffe et al., 2006). Among them, troponin complex regulates the muscle contraction, made up of three protein subunits: troponin I; inhibits binding of myosin with actin, troponin T; interact with tropomyosin, and troponin C; binds Ca^{2+} (Katrukha, 2013). Cardiac troponin I and T (cTnI and cTnT) shows high myocardial specificity and clinical sensitivity for MI (Daubert and Jeremias, 2010; Babuin and Jaffe, 2005), and remains in a bloodstream for prolonged time (Adams et al., 1993) as compared to other cardiac biomarkers. Therefore, they are considered as the gold standard in the MI diagnosis. The cTnI and cTnT can provide similar information about myocardial necrosis (Jaffe et al., 2006). However, cTnI shows small but significant superiority in diagnostic capability than cTnT in the early stage of MI (Gimenez et al., 2014). We used cTnI along with creatine kinase-MB isoform (CK-MB) and myoglobin proteins as the MI biomarkers in this work. Even though myoglobin and CK-

* Corresponding author.
E-mail address: hmcho@kriss.re.kr (H.M. Cho).

http://dx.doi.org/10.1016/j.bios.2016.08.049
0956-5663/

MB show insufficient myocardial specificity but their behavior can be use as a supportive information in early diagnosis and as an evidence of reinfarction.

Biosensors are broadly categorized based on optical and electrical transducing techniques. Electrochemical biosensors detect biological species in terms of change in conductance (Piao et al., 2014), capacitance (Lee et al., 2016), or impedance (Radhakrishnan et al., 2014) on interaction with sensor surface. Fabrication processes of the high-sensitive (hs) electrochemical sensor devices are complex, which need expensive setup such as clean-room (Ventra and Taniguchi, 2016; Ma et al., 2013; Lee et al., 2014). Surface plasmon resonance (SPR) based biosensor are the most studied (Homola, 2008; Park et al., 2014; Lapage et al., 2013) and commercialized (Biocore, 2016) optical biosensors. SPR technique was combined with photonic crystals (Zhang et al., 2014), waveguide (Jin et al., 2016), oxide nanostructures (Tereshchenko et al., 2016), and many other signal amplification methods (Qureshi et al., 2012) to increase their sensitivity and stability. Be as it may, SPR sensors suffer from ineluctable thermal noise (Nizamov and Mirsky, 2011) which restrict their use where low molecular weight and low concentration detection involved. The methods used for signal amplification and/or to suppress thermal noise makes device structure complex and expensive. There is a need of a simple and cost effective alternative with comparable sensitivity.

Here, we developed the first hs-cTnI direct assay SIS-based sensor. The sensing platform is based on the non-reflecting condition (NRC) for *p*-polarized wave (pseudo-Brewster angle) where ellipsometric angles (Ψ, Δ) are highly sensitive to the overlayer thickness. Simplicity is the best feature of SIS technology. The SIS sensor chip is just a spin-coted thin dielectric polymer layer on the silicon substrate, which can be functionalized to detect a variety of biomolecules such as peptides, proteins, and DNA via affinity binding.

2. Materials and methods

2.1. Chemicals

Silicon wafer with ⟨100⟩ orientation was purchased from MCL Electronics Materials, Ltd., China. 10-N-Boc-Amino-dec-1-ene (TBoc), hydrofluoric acid, trifluoroacetic acid (TFA), dichloromethane, ammonium hydroxide, ethanolamine, N-Hydroxysuccinimide (NHS), carboxymethyl dextran (CM-dextran) sodium salt, and human blood serum were purchased from Sigma-Aldrich Korea Ltd. 1-(3-Dimethylaminopropyl)-3-ethalcarbodimide hydrochloride (EDC) was from Tokyo Chemical Industry Co., Ltd. Phosphate buffer solution (PBS; 0.004 M phosphate buffer and 0.155 M NaCl, pH 7.4) was from Gibco, Thermo Fisher Scientific Korea Ltd. Cardiac troponin protein (cTnI-T-C) complex (from onwards referred to as a cTnI), human myoglobin protein and their corresponding monoclonal mouse antibodies were purchased from HyTest Ltd., Finland. Whereas human CK-MB protein was from Medix Biochemica Ltd., Finland and its monoclonal mouse antibody was from Biospecific Tech. Corp USA. All the chemicals were of analytical grade and used as received without further purification. Deionized (DI) water was used during the entire experiment.

2.2. SIS sensor chip fabrication

SIS sensor chips are Si wafers, coated with thin TBoc layer. We chose silicon because it is best for stable and homogeneous immobilization of bio-layer (DeBenedetti and Chabal, 2013; Tian and Teplyakov, 2012) which decide the sensor's performance (Mace et al., 2006; Escorihuela et al., 2014). Also, it is available with high chemical purity in any required size with a perfectly flat surface at a low cost. Eight-inch Si wafer was cleaned using conventional RCA cleaning procedure (Gale et al., 2008) before TBoc deposition. It contains four sequential steps. Briefly, first: removal of organic contaminants and particulates, second: removal of surface SiO_2 layer, third: metal ion cleaning, and fourth: rinsing and drying. Native SiO_2 layer from cleaned Si wafer was removed by wet etching using 1:20 mixture of hydrofluoric acid and DI water for about one min, which produces dihydride terminated Si surface (Aswal et al., 2006). Hydrogen-terminated Si surfaces are highly reactive and stable only for 10–20 min in air. A thin layer (3–5 nm) of TBoc polymer was spin-coated on the H-terminated Si surface and dried under UV radiation for two hours. The self-assembled monolayer (SAM) of TBoc attaches firmly to the Si surface via Si-C covalent bond. TBoc layer serves two purposes; prevents Si surface from oxidation and acts as an anchoring layer for other organic or biomolecules. Raw SIS sensor chips (11.5 mm × 11.5 mm, without dextran SAM) were diced from the TBoc coated eight-inch Si wafer, as shown in Fig. S1 in supplementary data. Raw SIS sensor chips have an excellent shelf life, more than two years.

2.3. Functionalization of SIS sensor chips

Raw SIS sensor chips were activated by removing tert-butoxy carbamate groups from the TBoc chains which expose amine groups over the sensor surface; detail process is in the literature (Strother et al., 2000). Shortly, raw SIS sensor chips were soaked in the solution of 25% TFA and 75% dichloromethane for 30 min, washed with DI water followed by soaking in 10% NH_4OH for 10 min and again washed with DI water. Activated raw SIS chips can be used directly as a sensor. However, they show low throughput because most of the binding sites are unavailable for antigen attachment due to random orientation of the polymer chains. Also, it is hard to alter the functionality of sensor surface for specific binding. Therefore, to maximize the amount of available binding sites, SAM of dextran was grown over the activated raw SIS chips by 12 h incubation in CM-dextran sodium salt solution (0.1 g/ml in PBS). Shelf-life of SIS sensor chips with dextran SAM is about two months.

SIS sensor chip was docked onto the sensor cell, shown in Fig. 1. Sensor surface was primed by flowing PBS until sensor signal stabilizes, takes nearly two min. Dextran SAM was activated using the 1:1 mixture of 0.4 M EDC and 0.1 M NHS. One milliliter solution of cTnI, CK-MB, and myoglobin antibodies were injected to functionalized the sensor surfaces for respective analyte detection. The immobilized antibody concentration was 25 µg/ml in PBS with pH = 4.5 and flow rate was 20 µl/min. Non-specific binding sites, i.e. non-reacted NHS esters were blocked by flowing 1 M ethanolamine solution for 10 min with the same flow rate. The immobilized surface was washed with PBS until sensor signal stabilizes, which removes loosely bounded and non-bounded antibody molecules. Stable SIS signal suggests sensor ready to measure.

Direct assays were used for all the binding experiments. Human cTnI, CK-MB, and myoglobin antigens were diluted in the pure PBS with different concentrations. One milliliter solution of each of these antigens was injected over the respective functionalized sensor surfaces, and binding events were measured. Injection flow rate was 100 µl/min and pH was 7.4. The cTnI samples in human blood serum were tested to demonstrate the capability of the SIS sensors in a real situation. Solutions of the cTnI in 10% human serum from 0.001 to 10 ng/ml concentrations were injected over sensor surface, and sensorgrams were measured.

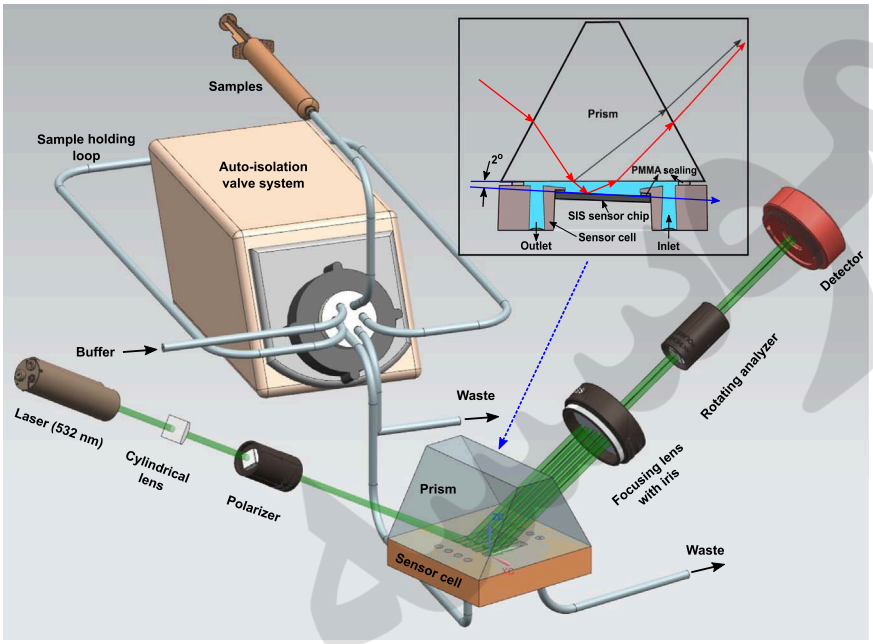

Fig. 1. Schematics of SIS sensor system. Ellipsometer in RAE configuration was used as an optical transducer to probe biomolecular interactions. Sensor chip was aligned at an inclination of 2° with respect to the surface of the prism to minimize the noise due to the reflected beam from the prism surface, shown in the inset.

2.4. SIS sensor system

SIS sensor system is a home-made multichannel device, can be section off as; sensor unit and optical transducer, schematics are shown in Fig. 1. Sensor unit includes liquid transport system and sensor assembly. Transport system consists of an auto-isolation valve to select proper liquid to flow, a pump, and the flow channels, which moves liquid to and fro from sensing area. Inset in Fig. 1 shows a cross-section of the sensor assembly, consists of a prism, sensor cell, and sensor chip, similar to the designed by Gao and Rothberg (2007). The sensor cell is a support structure for sensor chip and layout flow channels over the sensor chip. Reflected beam from prism surface is brighter than SIS signal (see inset of Fig. 1), and their interference gives a noisy signal. It is not possible to completely block the prism surface reflected beam due to narrow working space. This issue was addressed by applying 2° tilt to the sensor chip with respect to prism surface, shown in the inset of Fig. 1. Small inclination bends the SIS signal towards prism surface reflected beam so that they cross each other and become sufficiently apart (Rothberg, 2009).

Rotating analyzer ellipsometer (RAE) was used as the optical transducer, which facilitates two extremely surface sensitive parameters, ellipsometric angles (Ψ, Δ). In RAE configuration, optical components were arranged in order as: a light source, fixed polarizer, a cylindrical lens, SIS sensor assembly, focusing optics, rotating analyzer, and a detector, shown in Fig. 1. The light source was a diode laser with a central wavelength of 532 nm and average power of 25 mW. The cylindrical lens was used to convert a point source to a line source to access all the sensor channels in a single shot, which will provide the similar experimental environment. The detector was silicon diode. The RAE was mounted on the goniometer from Huber Corp., which can adjust NRC with 0.001° of accuracy.

3. Results and discussion

3.1. SIS principle

Ellipsometry is the most surface sensitive optical technique known today; measures change in polarization state of incident light upon interaction with the sample surface. Ellipsometry measures two parameters, Ψ and Δ simultaneously, which can provide more information about the system under study (Fujiwara, 2003). The Ψ and Δ are amplitude ratio and phase difference between p- and s-polarized light, and defined by complex reflectance ratio ρ as:

$$\rho = r_p/r_s = \tan(\Psi)\exp(i\Delta), \quad (1)$$

where, r_p and r_s are the complex reflection coefficients of p- and s-polarized light. Complex reflection coefficients are extremely sensitive to the overlayer thickness at Brewster angle (Azzam and Khan, 1983), it is advisable to measure near Brewster angle (Herzinger et al., 1998). The Ψ and Δ are expressed from Eq. (1) as:

$$\Psi = \tan^{-1}(|\rho|), \quad \Delta = \delta_p - \delta_s \quad (2)$$

SIS sensors operate at non-reflecting condition (pseudo-Brewster angle) for p-polarized wave, where Ψ shows extremely high sensitivity for thickness change of overlayer and Δ is almost constant (Diware et al., 2015). Therefore, we used Ψ as the sensing parameter which detects thickness variation due to analyte-antibody interactions.

SIS sensor performance was simulated by numerically calculating Fresnel coefficients (Fujiwara, 2003) for three layer optical model with PBS ambient, shown in Fig. 2a. Homogeneous and optically isotropic ambient/film/dielectric layer/substrate system was assumed for simulation. The dielectric layer (DL) is multilayer structure consists of antibody/dextran/TBoc layers. Refractive index of DL= 1.452 and buffer solution= 1.333 for green light (532 nm) were used for simulation. Inset of Fig. 2b shows the simulated Ψ signal with respect to the angle of incidence (AOI) for a given optical structure with 3 nm DL. The NRC position was at 72.185° where Ψ shows maximum sensitivity for growing thickness of biolayer. We observed that sensitivity of SIS sensor

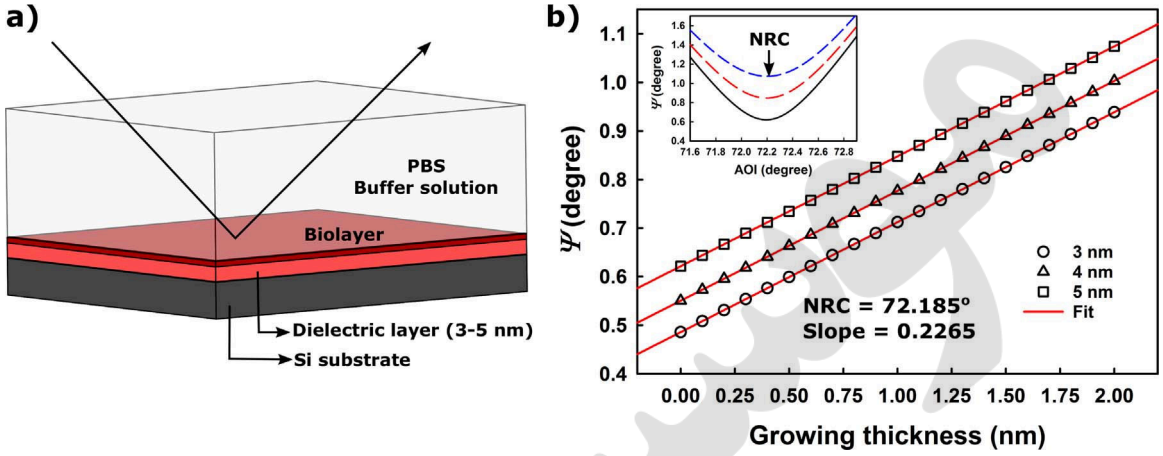

Fig. 2. Numerically simulated behavior of the SIS sensor. a) Three layer optical model with PBS buffer ambient was used for simulation. b) SIS signal (**Ψ**) with growing thickness of bio-layer for three different thicknesses of the dielectric layer, shows linear relation. The inset shows the NRC region where **Ψ** shows maximum sensitivity for thickness change.

depends on the thickness and uniformity of DL, which must be between 3 and 5 nm for optimum performance. The thickness of TBoc layer is the only factor that we can manipulate to control DL thickness and uniformity. Fig. 2b plots the simulation results for optimized SIS sensor structure; **Ψ** shows a linear dependence on the thickness of biolayer. The initial value of **Ψ** increases with DL's thickness, but its relation to the growing thickness of biolayer remains same. The change in **Ψ**, $d\Psi$, can directly correlate with the change in biolayer thickness (dT) at NRC, which translated as:

$$dT = \frac{1000}{0.2265} \times d_{\psi}\ pm \tag{3}$$

where, 1/0.2265 is a thickness translation factor, depends on the wavelength of probing light and 1000 is the scaling factor. It means one nm change in thickness will alter the value of **Ψ** by 0.2265 within the optimized conditions.

3.2. Sensor surface functionalization

The SIS sensor chips were functionalized for specific antigens binding, can be monitored and controlled in a real time. Fig. S2 shows the real time functionalization process for cTnI detection. The functionalization process begins with activation of dextran surface with EDC/NHS chemistry. The carboxyl groups on the CM-dextran SAM react with EDC and NHS to form an amine-reactive NHS ester, which increases the thickness by 76.5 pm over the sensor surface, shown in Fig. S2a. The cTnI antibody was immobilized over the activated dextran surface. Figure S2b shows the growth of 241.6 pm antibody layer through amine coupling. There would be some unreacted NHS ester molecules which could act as nonspecific binding sites, were blocked by injecting ethanolamine over the sensor surface. The cTnI antibody consumes most of the amine groups, confirmed by Fig. S2c. The change in RI will shift the NRC which affects the sensitivity of SIS sensors. As **Δ** signal is sensitive to the RI which can be used to monitor the state of a sensor in real time. The **Δ** signals are plotted along with the **Ψ** signal to monitor the stability of NRC position. The behavior of **Δ** signal also decides the length of washing phase before next measurement. Finally, functionalized sensor surface was primed with PBS until signal stabilizes, shown in Fig. S2d.

Fig. S3 shows the SIS responses for blank a) PBS and b) 10% human serum in PBS, measured at random time with various sensor chips. These background signals show no activity and are below the noise level of analyte signal. Therefore, there is no need of reference channel like SPR sensors, a one-time measurement of the blank buffer solution is enough to account the background noise. Diluted human serum signal shows slightly higher noise than PBS, may be due to the presence of scattering sites (heavy protein molecules).

3.3. Analyte binding analysis

We used direct assays for detection and quantification of MI biomarkers. Myoglobin, CK-MB, and cTnI samples were prepared with various concentrations between 1–1000, 0.1–2000, and 0.005–10 ng/ml, respectively in PBS, and injected over the respective functionalized sensor surface. Fig. 3a, b, and c show the representative SIS responses of the lowest measurable concentration of myoglobin, CK-MB, and cTnI. We were able to achieve the limit of detection (LOD) down to 1, 0.1 and 0.005 ng/ml for myoglobin, CK-MB, and cTnI, respectively. The LOD values are the statistical average of ten measurements. Our home-made SIS sensor system requires 5 min time frame for analyte detection which is comparable with the other techniques (Han et al., 2016). This response time will be less than 1 min with the sophisticated microfluidics.

Advancement in technology facilitates the progressive development of hs-cTnI immunosensors during last decades. Signal amplification techniques were applied to achieve high sensitivity, such as the use of nanostructured devices (Tuteja, 2014; Priyankaruppan et al., 2013; Shalev et al., 2013; Kong et al., 2012; Ko et. al., 2007; Song et. al., 2011) or sandwich assays assisted by heavy molecules or nano-particles (Jo et al., 2015; Kim et al., 2015; Singal et al., 2014; Sharma et al., 2013; Wu et al., 2010; Wei et al., 2003; Ylikotila et al., 2006; Todd et al., 2007; Dittmer et al., 2010; Cho et al., 2009). For example, Kim et. al. developed honeycomb structured silicon nanowire field-effect-transistor for cTnI detection and achieved the LOD of ~5 pg/ml (Kim et al., 2016). Also, single nanowire-based sensor gave the LOD of 0.25pg/ml (Lee et al., 2012). However, these sensor structures are complex, time-consuming, and not cost efficient. Fig. 4 shows the LOD of cTnI assay obtained in this work as compared with various sensor platforms from the literature. Our LOD values are above 99th percentile cutoff point in spite of a direct assay. As far as we know, there are no work reporting hs-cTnI sensor can cross the 99th percentile cutoff point without any amplification.

3.4. Analyte binding analysis in real situation

The binding features of cTnI samples prepared in the diluted

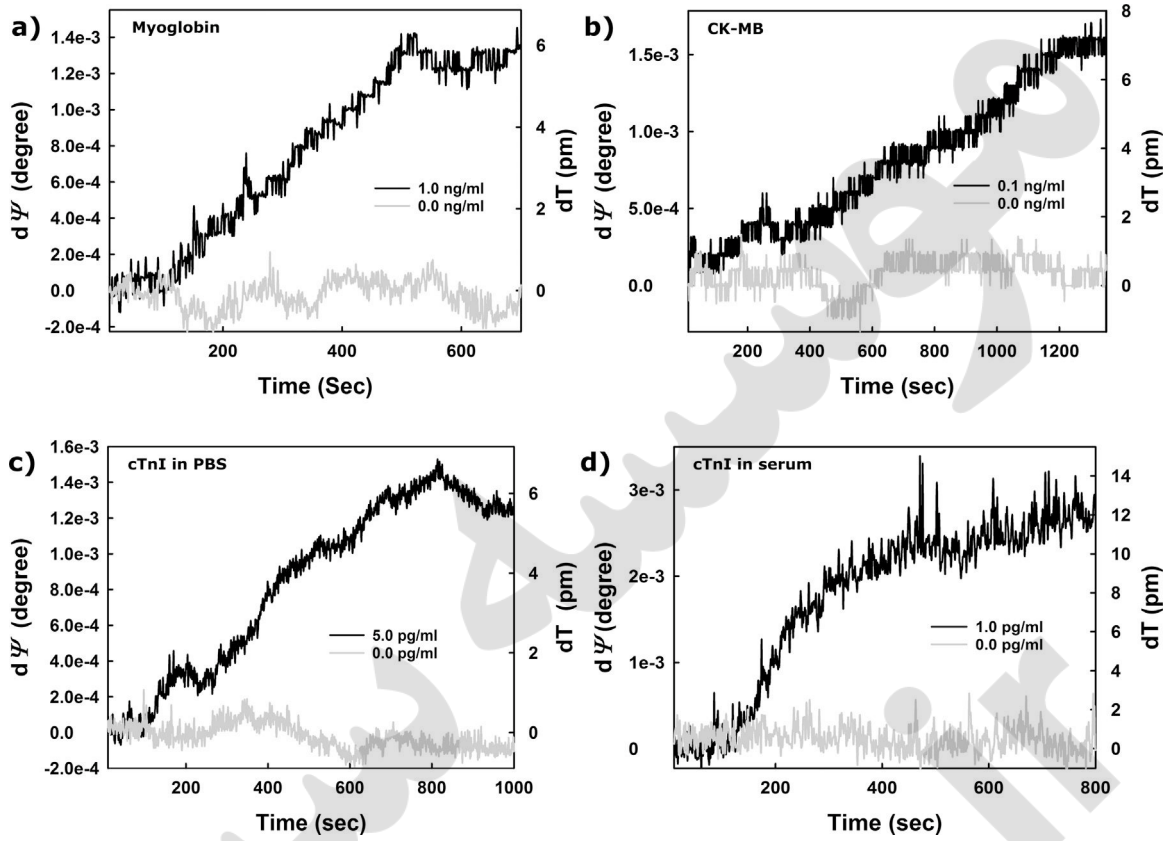

Fig. 3. Representative SIS profile of lowest measurable concentration of a) Myoglobin (1 ng/ml in PBS), b) CK-MB (0.1 ng/ml in PBS), c) cTnI (0.005 ng/ml in PBS), and d) cTnI (0.001 ng/ml in 10% human serum).

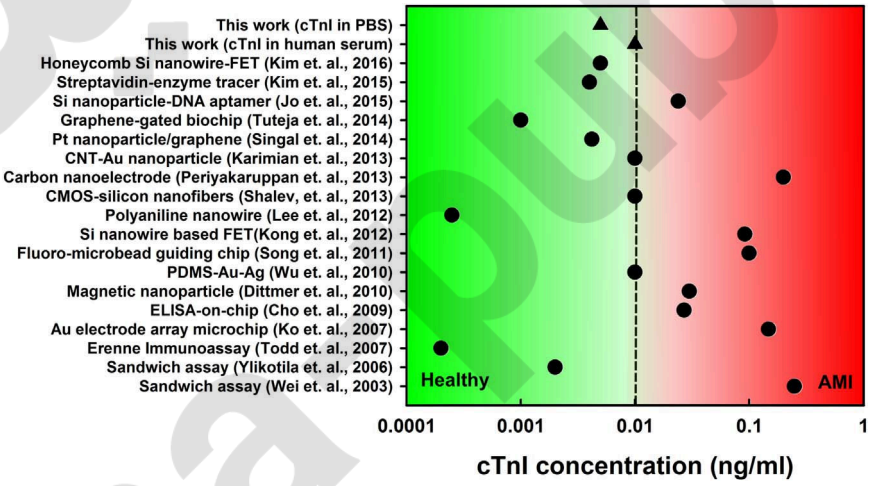

Fig. 4. Comparison of the LOD values for cTnI immunoassays reported in this work and previous work. Solid dash line is a 99th percentile cutoff point for several commercially available assays (Han et al., 2016). Solid triangles (▲) label our data.The LOD value for cTnI in 100% serum is extrapolated from cTnI in 10% serum data.

human serum (0.001–10 ng/ml) were investigated to study the effect of interfering protein molecules like in a real situation. The detection of cTnI protein in pure serum is not possible with current state of SIS sensor. Fig. 3d shows the SIS response for LOD (0.001 ng/ml) of cTnI in the diluted serum. The cTnI in serum shows fast and higher response than in PBS. It may be due to two possible reasons; non-specific binding and non-covalent association of heavy serum protein chain with cTnI molecules. However, blank serum response is flat (Fig. S3). More experimental evidence is needed to explain this behavior. For comparison, 100% serum data is extrapolated from 10% diluted serum data. As shown in Fig. 4, our LOD for cTnI in the 100% serum comes out to be 0.01 ng/ml, which is less than required current cTnI detection standard ~0.02 – 1 ng/ml) (Apple et al., 2012; Ramparany et al., 2011; Peacock et al., 2008).

Fig. 5 shows the concentration dependent SIS responses of myoglobin, CK-MB, and cTnI samples in PBS, and cTnI in human serum. These binding isotherms are also known as calibration plots, show typical behavior. Each data point is the statistical average of ten measurements with the standard deviation (SD) of ±5% for myoglobin and CK-MB, ±8% for cTnI in PBS, and ±10 – 12% for cTnI in diluted serum. The biolayer thickness gradually increases with MI biomarkers concentration and reaches to plateau at saturation. Growing biolayer thickness shows logarithmic

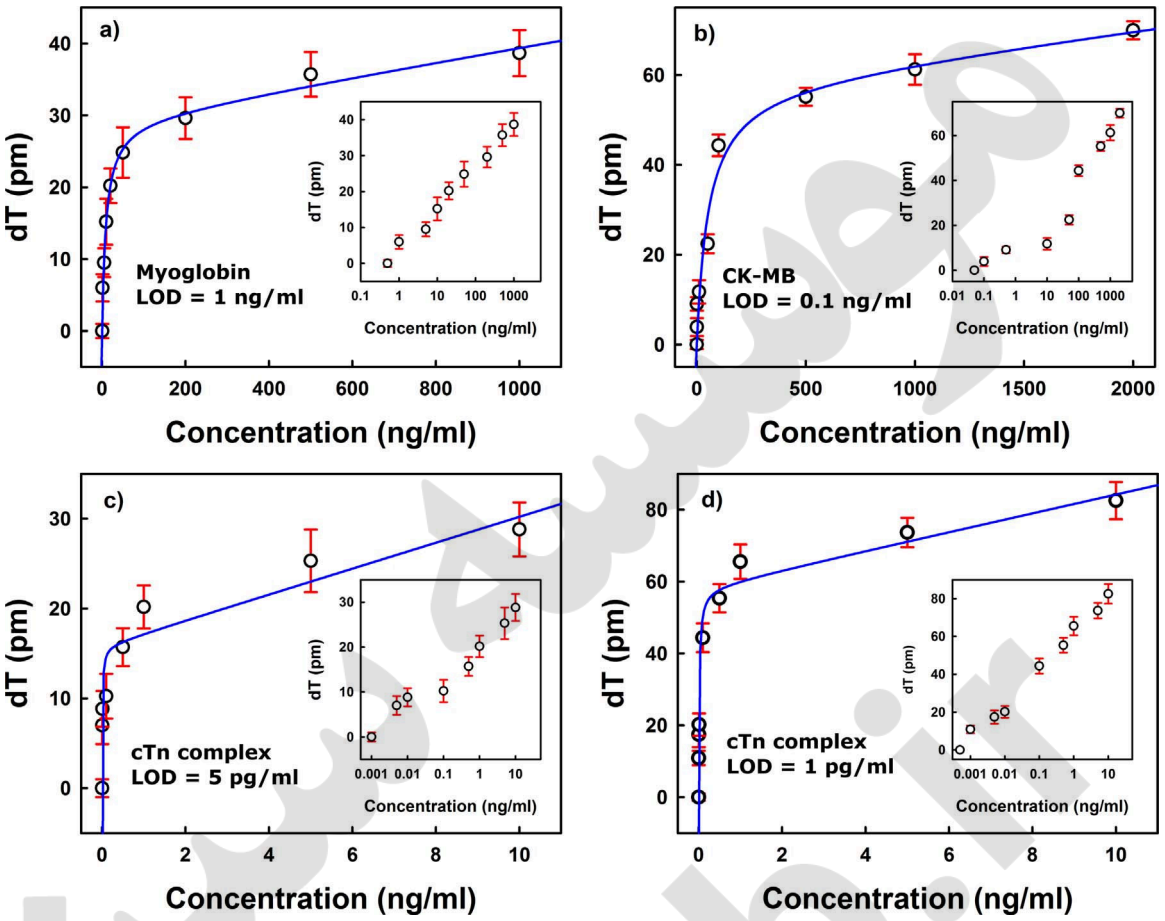

Fig. 5. Calibration plots of SIS sensors for a) myoglobin, b) CK-MB, c) cTnI in PBS buffer solution, and d) cTnI in 10% human serum. Each measurement is repeated ten times with SD of ±5% for myoglobin and CK-MB, ±8% for cTnI in PBS, and ±10 – – 12% for cTnI in diluted serum. The fitting curve (solid line) represents specific (major) and non-specific (minor) contributions to the calibration curves of SIS sensors. Inset: SIS responses with the analyte concentration in logarithmic scale.

dependence over measured concentration range while linear in the low analyte concentration range. Plateau regions of the calibration plots are not flat; small inclination suggests there may be some non-specific binding involved. The calibration plots were modeled by considering major specific and minor non-specific binding:

$$dT = \frac{B_{max} \cdot C}{K_D + C} + K_{ns} \cdot C \quad (4)$$

where, B_{max} is the maximum number of available binding sites, K_D is the equilibrium dissociation constant, K_{ns} is a binding constant for non-specific attachment, and C is the concentration of the analyte. Non-linear regression fitting routing was used to fit data. The cTnI in serum samples shows considerably higher non-specific components than PBS, which may explain higher binding response. We believe that SIS sensors can perform much better with sophisticated microfluidics and sensor chip fabrication process.

4. Conclusion

In conclusion, an ultra-sensitive, fast and cost effective optical SIS sensors were fabricated for diagnosis of MI. SIS sensor chip is a thin dielectric polymer layer coated Si wafer, functionalized with antibody and immersed in a liquid contains respective target species. The SIS sensor operates at NRC and monitors changes in the Ψ and Δ signals, which show high sensitivity for growing thickness due to antibody-antigen interactions and RI change of buffer solution, respectively. We were able to achieve the LOD of 1 ng/ml for myoglobin, 0.1 ng/ml for CK-MB, 0.005 ng/ml for cTnI in PBS, and 0.01 ng/ml for cTnI in human serum without the use of any tagging or labeling. The SIS sensors show a linear dependence on analyte concentration between 0.1–100 ng/ml for myoglobin and CK-MB, 0.005–1 ng/ml for cTnI in PBS, and 0.01–10 ng/ml for cTnI in human serum. The sensor chips are robust whose surface could be regenerated for reuse (not included in this work), which can further reduce the operation cost. High sensitivity and short response time for detection of cTnI in real human serum are necessary for the diagnosis of MI, which proves SIS technology have great potential in the point-of-care application. Present works may initiate the development of SIS sensors for other diseases diagnosis, food safety, environment monitoring, and drug discovery.

Acknowledgments

Financial support for this work was from the Industrial Strategic Technology Development Program (Grant No. 10064060) funded by the Ministry of Trade, Industry & Energy (MI, Korea).

Appendix A. Supplementary data

Supplementary data associated with this article can be found in the online version at http://dx.doi.org/10.1016/j.bios.2016.08.049.

References

Adams, J.E., Adendschein, D.R., Jaffe, A.S., 1993. Circulation 88 (2), 750–763.
Ahmed, A.H., Shankar, K.J., Eftekhari, H., Munir, M.S., Robertson, J., Brewer, A., Stupin, I.V., Casscells, S.W., 2007. Exp. Clin. Cardiol. 12, 189–196.
Ahmed, N., Carrick, D., Layland, J., Oldroyd, K.G., Berry, C., 2013. Heart Lung Circ. 22, 243–255.
Apple, F.S., Ler, R., Murakami, M.M., 2012. Clin. Chem. 58, 1574–1581.
Aswal, D.K., Lenfant, S., Guerin, D., Yakhmi, J.V., Vuillaume, D., 2006. Anal. Chim. Acta 586, 84–108.
Azzam, R.M.A., Khan, M.E.R., 1983. Appl. Opt. 22, 4155–4166.
Babuin, L., Jaffe, A.S., 2005. CMAJ 173 (10), 1191–1202.
Biocore, 2016. General Electric company.⟨https://www.biacore.com/lifesciences/introduction/index.html⟩.
Cho, I., Peak, E., Kim, Y., Kim, J., Peak, S., 2009. Anal. Chim. Acta 632, 247–255.
Daubert, M.A., Jeremias, A., 2010. Vasc. Health Risk Manag. 6, 691–699.
DeBenedetti, W.J.I., Chabal, Y.J., 2013. J. Vac. Sci. Technol. A 31, 050826.
Diware, M.S., Cho, H.M., Chegal, W., Cho, Y.J., Jo, J.H., O, S.W., Paek, S.H., Yoon, Y.H., Kim, D., 2015. Analyst 140, 706–709.
Dittmer, W.U., Evers, T.H., Hardeman, W.M., Huijnen, W., Kamps, R., Kievit, P., Neijzen, J.H.M, Nieuwenhuis, J.H., Sijbers, M.J.J., Dekkers,, D.W.C., Hefti, M.H., Martens, M.F.W.C., 2010. Clin. Chim. Acta 411, 868–873.
Escorihuela, J., Banuls, M., Rosa Puchades, R., Maquieira, A., 2014. J. Mater. Chem. B 2, 8510–8517.
Fujiwara, H., 2003. Spectroscopic Ellipsometry: Principles and Applications. John Wiley& Sons Ltd., Chichester.
Gale, G.W., Small, R.J., Reinhardt, K.A., 2008. Overview of aqueous cleaning, rinsing, and drying applications and techniques. In: Reinhardt, K.A., Kern, W. (Eds.), Handbook of Silicon Wafer Cleaning Technology, 2nd ed. Elsevier, New York, pp. 201–265.
Gao, T., Rothberg, L.J., 2007. Anal. Chem. 79, 7589–7595.
Gimenez, M.R., Twerenbold, R., Reichlin, T., Wildi, K., Haaf, P., Schaefer, M., Zellweger, C., Moehring, B., Stallone, F., Sou, S.M., Mueller, M., Denhaerynck, K., Mosimann, T., Reiter, M., Meller, B., Freese, M., Stelzig, C., Klimmeck, I., Voegele, J., Hartmann, B., Rentsch, K., Osswald, S., Mueller, C., 2014. Eur. Heart J. 35, 2303–2311.
Gutterman, D.D., 2009. Circ. J. 73, 785–797.
Han, X., Li, S., Peng, Z., Othman, A.M., Leblanc, R., 2016. ACS Sens. 1, 106–114.
Herzinger, C.M., Johs, B., McGahan, W.A., Woollam, J.A., 1998. J. Appl. Phys. 83, 3323–3336.
Homola, J., 2008. Chem. Rev. 108, 462–493.
Janota, T., 2014. Coe et Vasa 56, e304–e310.
Jaffe, A.S., Babuin, L., Apple, F.S., 2006. J. Am. Coll. Cardiol. 48, 1–11.
Jo, H., Gu, H., Jeon, W., Youn, H., Her, Jin., Kim, S., Lee, J., Shin, J.H., Ban, C., 2015. Anal. Chem. 87, 9869–9875.
Jin, Z., Guan, W., Lin, C., Xue, T., Wang, Q., Zheng, W., Cui, X., 2016. Appl. Phys. Sci. 377, 207–212.
Katrukha, I.A., 2013. Biochemistry (Moscow) 78, 1447–1465.
Kim, K., Chanoh, P., Kwon, D., Kim, D., Meyyappan, M., Jeon, S., Lee, J., 2016. Biosens. Bioelectron. 77, 695–701.
Kim, G., Seo, S., Peak, S., Kim, S., Jeon, J., Kim, D., Cho, I., Peak, S., 2015. Sci. Rep. 5, 14848.
Kong, T., Su, R., Zhang, B., Zhang, Q., Cheng, G., 2012. Biosens. Bioelectron. 34, 267–272.
Ko, S., Kim, Bumjun, Jo, S., Oh, S., Park, J., 2007. Biosens. Bioelectron. 23, 51–59.
Lee, S.M., Han, N., Lee, R., Choi, I., Park, Y., Shin, J., Yoo, K., 2016. Biosens. Bioelectron. 77, 56–61.
Lee, J., Dak, P., Lee, Y., Park, H., Choi, W., Alam, M., Kim, S., 2014. Sci. Rep. 4, 7352.
Lee, I., Luo, X., Huang, J., Cui, X.T., Yun, M., 2012. Biosensors 2, 205–220.
Lapage, D., Jimenez, A., Beauvais, J., Dubowski, J.J., 2013. Light-Sci. Appl. e62, 1–8.
Ma, H., Wallbank, R.W.R., Chaji, R., Suzuki, Li J., Jiggins, C., Nathan, A., 2013. Sci. Rep. 3, 2730.
Mace, C.R., Striemer, C.C., Miller, B.L., 2006. Anal. Chem. 78, 5578–5583.
Nizamov, S., Mirsky, V.M., *Biosens. Bioelectron* 2011 **28** 263–269.
Piao, Y., Han, D.J., Seo, T.S., 2014. Sens. Actuators B Chem. 194, 454–459.
Park, B., Yun, S.H., Cho, C.Y., Kim, Y.C., Shin, J.C., Jeon, H.G., Huh, Y.H., Hwang, I., Baik, K.Y., Lee, Y.I., Uhm, H.S., Cho, G.S., Choi, E.H., 2014. Light-Sci. Appl. e222, 1–8.
Priyankaruppan, A., Gandhiraman, R.P., Meyyappan, M., Koehne, J.E., 2013. Anal. Chem. 85, 3868–3863.
Peacock, W.F., DeMarco, T., Fonarow, G.C., Diercks, D., Wynne, J., Apple, F.S., Wu, A. H., 2008. New Engl. J. Med. 358, 2117–2126.
Qureshi, A., Gurbuz, Y., Niazi, J.H., 2012. Sens. Actuators B Chem. 117–172, 62–76.
Radhakrishnan, R., Suni, I.I., Bever, C.S., Hammock, B.D., 2014. ACS Sustain. Chem. Eng. 7, 1649–1655.
Richard, C.C., Bavry, A.A., Petersen, J.W., 2012. J. Am. Coll. Cardiol. 59, 435–441.
Ramparany, L., Ramirez, J., Nizou, J., Saux, D.L., Richand, V., Talarmin, A., 2011. Clin. Vaccin. Immunol. 18, 414–417.
Sharma, R.V., Puri, N.K., Singh, R.K., Biradar, A.M., Mulchanadani, A., 2013. Appl. Phys. Lett. 103, 203703.
Rothberg, L.J., 2009. U. S. Patent US 7551294 B2.
Singal, S., Shrivastava, A.K., Biradar, A.M., Mulchandani, A., Rajesh,*Sens and Actuators B* **205**, 2014 363–370.
Shalev, G., Landman, G., Amit, I., Rosenwaks, Y., Levy, I., 2013. NGP Asia Mater. 5, e41.
Song, S.Y., Han, Y.D., Kim, K., Yang, S.S., Yoon, H.C., 2011. Biosens. Bioelectron. 26, 3818–3824.
Strother, T., Hamers, R.J., Smith, L.M., 2000. Nucleic Acids Res. 28, 3335–3541.
Tereshchenko, A., Bechelany, M., Viter, R., Khranovskyy, V., Smyntyna, V., Starodub, N., Yakimova, R., 2016. Sens. Actuators, B 229, 664–677.
Tian, F., Teplyakov, A.V., 2012. Langmuir 29, 13–28.
Todd, J., Freese, B., Lu, A., Held, D., Morey, J., Livingston, R., Goix, P., 2007. Clin. Chem. 53, 1990–1995.
Tuteja, S.K., Priyanka, Bhalla, V., Deep, A., Paul, A.K., Suri, C.R., 2014. Anal. Chim. Acta. 809, 148–154.
Ventra, M.D., Taniguchi, M., 2016. Nat. Nanotechnol. 11, 117–126.
Wu, W., Bian, Z., Wang, W., Zhu, J., 2010. Sens. Actuators B 147, 298–303.
Wei, J.W., Mu, Y., Song, D., Fan, X., Jiu, X., Bu, L., Zhang, H., Zhnag, G., Ding, J., Wang, W., Jin, Q., Luo, G., 2003. Anal. Biochem. 321, 209–216.
WHO, 2015. Cardiovascular diseases. World Health Organization. ⟨http://www.who.int/mediacentre/factsheets/fs317/en/⟩(updated January 2015).
Ylikotila, J., Hellstrom, J.L., Eriksson, S., Vehniainen, M., Valimaa, L., Takalo, H., Bereznikova, A., Pettersson, K., 2006. Clin. Biochem. 39, 843–850.
Zhang, B., Morales, A.W., Peterson, R., Tang, L., Ye, J.Y., 2014. Biosens. Bioelectron. 58, 107–113.